





An experimental and theoretical study of two pyridinium salt derivatives as API 5L Grade B steel corrosion inhibitors in H₂SO₄ solution

B. Mezhoud,^{1,2} * A. Bouraiou,¹  M.E. Said,^{1,3}  A. Kherrouba,⁴ 
D. Hannachi^{5,6} and A. Chibani¹

¹Unit for Environmental Chemistry and Molecular Structural Research, CHEMS, University of Frères Mentouri Constantine 1, Constantine, Algeria

²Department of Chemistry, Faculty of Exact Sciences and Computer Science, Mohamed Sedik Ben Yahia University, B.P 98 Ouled Aissa, 18000, Jijel, Algeria

³Faculty of Technology, Mohamed Boudiaf University, B.P 166 Ichbelia, 28000, M'sila, Algeria

⁴Materials Chemistry Laboratory Constantine, University of Frères Mentouri Constantine 1, Constantine, Algeria

⁵Laboratory of Electrochemistry, Molecular Engineering and Redox Catalysis (LEIMCR), Department of Basic Education in Technology, Faculty of Technology, University Ferhat Abbas, Setif-1, Algeria

⁶Department of Chemistry, Faculty of Mterial Science, University of Batna-1, Batna, Algeria

*E-mail: bilelmezhoud@univ-jijel.dz

Abstract

The inhibition of API 5L Grade B steel corrosion in sulfuric acid solution in the presence of some pyridinium salt derivatives such as 1,1'-methylenebis(pyridin-1-ium)bromide (pyridinium salt **1**) and 1,1'-(ethane-1,2-dyl))bis(pyridin-1-ium)bromide (pyridinium salt **2**) was conducted using weight loss techniques, potentiodynamic polarization methods, electrochemical impedance spectroscopy (EIS), atomic force microscopy (AFM) and theoretical calculations. Various parameters were determined and discussed to fully understand the mode of action of these compounds, including thermodynamic activation, adsorption, and quantum chemical parameters. The results obtained by all techniques revealed that these derivatives are suitable inhibitors for this type of steel in sulfuric acid solutions. In addition, the inhibition efficiency increases with pyridinium salt concentration and temperature. The polarization curves show that both pyridinium salts are mixed-type inhibitors. Electrochemical impedance spectroscopy (EIS) indicates that charge transfer controls the corrosion process of steel in the absence and presence of compounds. The adsorption of each compound occurs via electrostatic and chemical bonds and obeys Langmuir's adsorption isotherm. AFM images demonstrate that these salts protect this steel in H₂SO₄ solution. Theoretical calculations indicate a correlation between the experimental and quantum parameters.

Keywords: *steel corrosion, sulfuric acid solution, pyridinium salts, potentiodynamic polarisation.*

1. Introduction

Metals, particularly ferrous metals, play a crucial role in our daily lives due to their excellent mechanical properties and affordability. They are utilized in various industrial and engineering applications [1]. Before these metals are ready for use in various activities, they undergo different processes such as acid pickling, painting, laminating, galvanizing, and electroplating. In acid pickling processes, the metal part is immersed in a suitable acid solution, known as an acid pickling bath, to remove unwanted scale and rust from metal surfaces. Once the scale and rust have dissolved, the metal is exposed to further acid attack and corrodes. The aggressive behavior of the acid requires corrosion inhibitors, which are essential to limit the acid attack. The most commonly used inhibitors in acidic environments are organic. These inhibitors can adhere well to the metal surface and form a protective layer that shields the metal from aggressive acids. Compounds containing nitrogen, sulfur, oxygen, phosphorus, and aromatic heterocyclic systems with conjugated double- or triple-bond structures have been proven to be highly effective inhibitors of metal corrosion, particularly in acidic environments [2–9]. The efficiency of an inhibitor primarily relies on its ability to adsorb onto the metal surface, displacing water molecules and forming a layer at the interface [10, 11]. In general, the adsorption of organic inhibitors on the metal surface is described by two main interaction types: physical adsorption and chemisorption, dependent on the metal charge and its nature, the organic compound's chemical structure, and the electrolyte type [12]. Several studies have shown that organic salt compounds exhibit important features as corrosion inhibitors, mainly attributable to the synergistic interaction between the organic cations and the halide anions [13–19]. This research is dedicated to evaluating the inhibitory properties of two pyridinium salt derivatives on API 5L Grade B steel in H_2SO_4 solution.

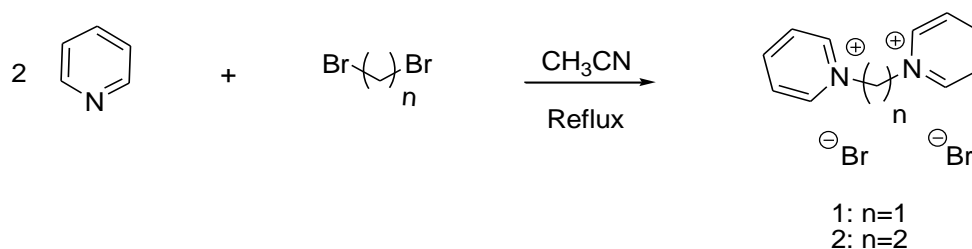
2. Experimental

2.1. Sample preparation and solution

The corrosion tests were conducted on API 5L Grade B steel samples with the following composition (wt.%): C (0.28), Mn (1.20), S (0.03), Cr (0.50), Cu (0.50), and Fe balance. The samples utilized for the weight loss test and surface analysis were cut into cubes with an area ranging from 5 to 6 cm^2 . The working electrode utilized in the electrochemical tests had an exposed area of 0.265 cm^2 as a square. All steel samples were mechanically abraded with grade emery papers (220, 400, 600, 800, 1200, and 2000 grade), rinsed with distilled water, degreased in acetone, and dried at room temperature. The corrosive medium used in this study was prepared from a commercial solution of sulfuric acid (95–97%) and distilled water.

2.2. Inhibitors

The preparation of pyridinium salt **1** and **2** was carried out by the reaction of two equivalents of pyridine and one equivalent of dibromomethane and dibromoethane, respectively. The mixture was heated at reflux for 24 hours in acetonitrile to give the desired salts **1** and **2** with 79% and 88% of yields, respectively. The reaction is represented in Scheme 1:



Scheme 1. Preparation of inhibitors **1** and **2**.

2.2.1. Experimental protocol

A mixture of 2 mmol of 1,2-dibromoalkane derivative (dibromomethane or dibromoethane) and 5 mmol of pyridine in 20 mL of acetonitrile was refluxed for 24 hours. After cooling at -20°C , the obtained precipitate was filtered, washed several times with acetonitrile and vacuum-dried. The structures of both compounds were established using spectroscopic methods, and the obtained data are in good accordance. The obtained solids were used without any further purification.

Compound 1: Yield 79%; white solid; mp. $>270^{\circ}\text{C}$; ^1H NMR (250.13 MHz, D_2O): $\delta=9.23$ (d, $J=6.3$ Hz, 4H), 8.72 (t, $J=7.7$ Hz, 2H), 8.19 (t, $J=6.8$ Hz, 4H), 7.33 (s, 2H) ppm.

Compound 2: Yield=88%; white solid; mp. $>270^{\circ}\text{C}$; ^1H NMR (250.13 MHz, D_2O): $\delta=8.77$ (d, $J=6.5$ Hz, 4H), 8.59 (t, $J=7.8$ Hz, 2H), 8.04 (t, $J=6.7$ Hz, 4H), 5.26 (s, 4H) ppm.

2.3. Weight loss measurements

Once the preparation of steel specimens was completed, each sample was weighed and immediately immersed in solution containing 0.5 M H_2SO_4 , with and without different concentrations of compounds for 4 hours at 25°C . When the exposure time was over, the samples were removed from the solution, cleaned with distilled water to remove the corrosion products deposited on the surface. After rinsing and drying, the samples were reweighed.

2.4. Electrochemical measurements

Electrochemical measurements were realized in a three-electrode cell at 25°C using a Gamry Instruments potentiostat/galvanostat/ZRA (Reference 3000). A platinum wire was employed as a counter electrode, and a saturated calomel electrode (SCE) was used as a reference electrode. The cell was placed in a water thermostat to get the necessary temperature. Before plotting the polarization curves and electrochemical impedance diagrams, the working

electrode was immersed in the test solution for 30 minutes at open circuit potential (OCP) to obtain a steady state. The polarization curves of the metal solution interface were obtained in potentiodynamic mode by varying the potential continuously from -800 to -200 mV towards ECS with the scan rate of 1 mV/s. The EIS measurements were performed at OCP in the 10 mHz – 100 kHz frequency range using a sinusoidal AC perturbation with an amplitude of 10 mV peak-to-peak.

2.5. Atomic Force Microscopy (AFM)

Atomic force microscopy (AFM) was used to characterize the surface topography of the steel sample before and after 4 h immersion in 0.5 M H_2SO_4 solution without and with 7.5×10^{-3} M of inhibitors with a PicoScan AFM in tapping mode over two $3\mu \times 3\mu$.

2.6. Theoretical examination

The Gaussian 09 program is used to optimize the geometries of the molecules studied and to calculate their frequencies. These calculations are carried out using the DFT method with the B3LYP functional on the standard 6-31G (d,p) basis. The quantum chemical parameters obtained were EHOMO, ELUMO, and ΔE and dipole moment (μ).

3. Results and Discussion

3.1. Weight loss studies

In order to evaluate the protective effect of pyridinium salts 1 and 2 on the corrosion performance of API 5L Grade B steel in 0.5 M H_2SO_4 solution, we performed gravimetric measurements of API 5L grade B steel without and with different concentrations of inhibitors. The corrosion rate (W), surface coverage (θ), and inhibition efficiency ($IE\%$) are determined after 4 hours of immersion at 25°C . The following relations calculate the corrosion parameters of weight loss measurements:

$$IE\% = \frac{W_0 - W_{\text{inh}}}{W_0} \times 100 \quad (1)$$

$$W = \frac{\Delta m}{S \cdot t} \quad (2)$$

$$\theta = \frac{W_0 - W_{\text{inh}}}{W_0} \quad (3)$$

where W_0 and W_{inh} represent the corrosion rates of steel in the absence and presence of inhibitors, respectively; Δm denotes the corrosion weight loss of steel (in grams); t signifies the exposure time of samples in hours, and S represents the surface area of the steel samples in square meters. The corrosion parameters from weight loss measurements in 0.5 M H_2SO_4 solution with various inhibitor concentrations at 25°C are presented in Table 1.

Table 1. Corrosion parameters obtained from weight loss measurements for API 5L Grade B steel in 0.5 M H₂SO₄ solution without and with different concentration of pyridinium salts for 4 hours at 25°C.

Inhibitor	Concentration, M	$V, \text{g} \cdot \text{m}^2 \cdot \text{h}^{-1}$	$IE, \%$	θ
Blank	0.5	9.77	—	—
	5×10^{-4}	3.10	68.27	0.68
	1×10^{-3}	1.85	81.06	0.81
	5×10^{-3}	0.88	90.94	0.90
Inhibitor I	7.5×10^{-3}	0.87	91.10	0.91
	5×10^{-4}	3.01	69.19	0.69
	1×10^{-3}	2.02	79.32	0.79
Inhibitor II	5×10^{-3}	1.19	87.81	0.87
	7.5×10^{-3}	0.92	90.57	0.90

It is evident from Table 1 that as the concentration of pyridinium salts in the acid solution increases from 0 to 7.5×10^{-3} M, the corrosion rate decreases, and the inhibition efficiency significantly improves. This suggests that the amount of adsorption and coverage on the metal surface by the inhibitor increases with the rising concentration [20]. The inhibitors are very effective at a concentration of 7.5×10^{-3} M. This is probably because the inhibitors' molecules cover the whole metal surface. It is also noted that adding an extra CH₂ group between the two pyridinium salts in the second compound does not significantly change how well it inhibits.

3.2. Potentiodynamic polarization curves

The polarization curves of API 5L Grade B steel submerged in H₂SO₄ 0.5 M at 25°C and without and with different concentrations of inhibitors I and II are presented in Figure 1.

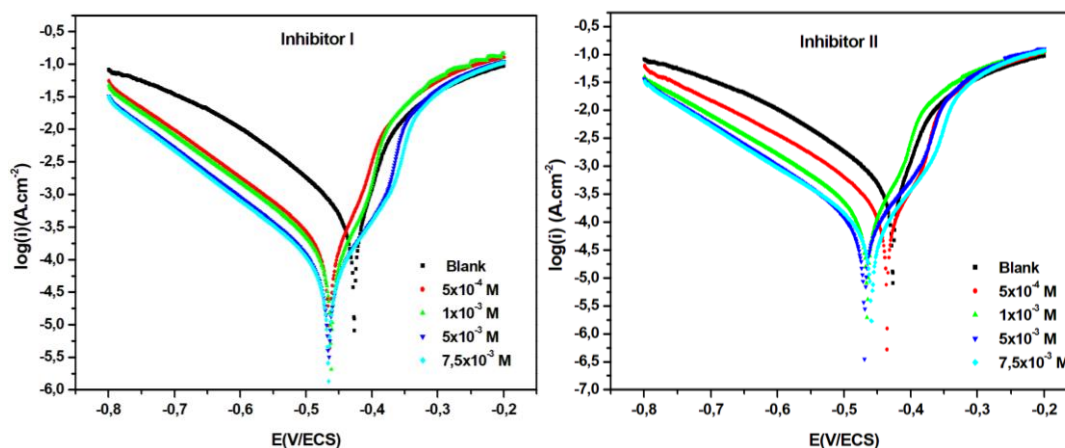
**Figure 1.** Polarization curves of API 5L Grade B steel in 0.5 M H₂SO₄, without and with different concentration of pyridinium salts I and II at 25°C.

Figure 1 shows that adding pyridinium salts to the corrosive medium shifts the anodic and cathodic Tafel lines to lower current density values. However, this shift is more significant in the cathodic region, suggesting that these salts inhibit the reduction of hydrogen ions more than the anodic dissolution. The extent of this decrease depends on the concentration of the inhibitors, attributed to the adsorption of the inhibitors on the steel surface and subsequent blocking of active sites [21–24]. It can also be observed that as the polarization potential tends toward a more positive value, the desorption of the inhibitors becomes evident, leading to a significant increase in the corrosion current density compared to the initial phase of anodic scanning [16, 25]. In the cathodic domain, the curves are parallel and show a sizable linear segment, indicating that Tafel's law is verified and that hydrogen reduction is controlled by pure activation kinetics [26, 27]. Various electrochemical parameters were measured to obtain information about the corrosion kinetics. These parameters include the corrosion potential (E_{corr}), the cathodic (b_c) and anodic (b_a) Tafel slopes, the corrosion current density (i_{corr}), linear polarization resistance (LPR), the surface coverage (θ), and the inhibition efficiency ($IE\%$). These values were obtained by extrapolating the polarization curve using the Tafel method. These parameters are listed in Table 2. The following equations were also used to calculate the inhibition efficiency ($IE\%$) and the surface coverage (θ):

$$IE\% = \frac{i_{\text{corr}}^0 - i_{\text{corr}(i)}}{i_{\text{corr}}^0} \times 100 \quad (4)$$

$$\theta = \frac{i_{\text{corr}}^0 - i_{\text{corr}(i)}}{i_{\text{corr}}^0} \quad (5)$$

where $i_{\text{corr}(i)}$ represents the corrosion current density at a particular amount of pyridinium salts, whereas i_{corr}^0 represents the corrosion current density without pyridinium salts.

Table 2. Electrochemical parameters of API 5L Grade B steel in H_2SO_4 0.5 M medium in the absence and presence of different concentrations of inhibitors at 25°C.

	C_{inh}, M	$-E_{\text{corr}}, \text{mV}$	$i_{\text{corr}}, \mu\text{A}\cdot\text{cm}^{-2}$	$b_c, \text{mV}\cdot\text{dec}^{-1}$	$b_a, \text{mV}\cdot\text{dec}^{-1}$	$LPR, \text{Ohm}\cdot\text{cm}^2$	$IE\%$	θ
Blank	0.5	427	871.69	178.1	100.1	31.92	–	–
	5×10^{-4}	463	229.05	146.1	87.70	103.89	73.72	0.73
Inh I	1×10^{-3}	462	160.00	140.3	81.50	139.90	81.64	0.81
	5×10^{-3}	466	75.09	128.1	77.70	279.67	91.38	0.91
	7.5×10^{-3}	466	70.56	128.5	77.60	297.73	91.90	0.91
	5×10^{-4}	436	226.41	147.0	80.60	99.83	74.02	0.74

	C_{inh}, M	$-E_{\text{corr}}, \text{mV}$	$i_{\text{corr}}, \mu\text{A}\cdot\text{cm}^{-2}$	$b_{\text{c}}, \text{mV}\cdot\text{dec}^{-1}$	$b_{\text{a}}, \text{mV}\cdot\text{dec}^{-1}$	$LPR, \text{Ohm}\cdot\text{cm}^2$	$IE\%$	θ
	1×10^{-3}	465	198.49	147.1	87.90	120.36	77.22	0.77
Inh II	5×10^{-3}	470	90.18	128.0	79.20	235.58	89.65	0.89
	7.5×10^{-3}	459	78.11	131.7	75.50	266.77	91.03	0.91

The results presented in Table 2 reveal that the addition of various concentrations of pyridinium salts to the corrosive medium causes a random shift in the corrosion potentials values towards the negative direction. This shift, in comparison to H_2SO_4 , is less than 85 mV (approximately -43 mV), indicating that these inhibitors act as mixed inhibitors with a predominantly cathodic effect [3, 28]. It is noteworthy that both the inhibition efficiency and the surface coverage (θ) increase with the concentration of pyridinium salts, reaching a maximum value of 91.90% for Inhibitor I and 91.03% for Inhibitor II at a concentration of 7.5×10^{-3} M. Furthermore, the addition of varying concentrations of inhibitors to the corrosive medium modifies the anodic and cathodic slopes. This implies that inhibitor molecules are adsorbed on both anodic and cathodic active sites, indicating that these inhibitors exert control over both cathodic and anodic reactions [14].

3.4. Electrochemical impedance spectroscopy

To gain deeper insights into the mechanisms of corrosion prevention, electrochemical impedance spectroscopy (EIS) measurements were performed on API 5L Grade B steel immersed in H_2SO_4 solution with and without the presence of synthesized pyridinium salts. In Figure 2, Nyquist diagrams depict the behavior of steel in 0.5 M H_2SO_4 with pyridinium salts I and II at 25°C. The shape of the Nyquist diagram exhibits a depressed capacitive loop, indicating that the corrosion process of API 5L Grade B steel in these solutions is controlled by the transfer of charge [29–31]. The depression in the semicircular loop is commonly associated with the roughness and heterogeneity of the steel surface [32]. The diameter of the capacitive loop progressively increases with a rise in inhibitor concentration, suggesting the adsorption of inhibitor molecules. This phenomenon creates a barrier that effectively shields the metal from aggressive attacks in the solution [33, 34].

The parameters pertaining to the electrochemical impedance measurements of steel in 0.5 M H_2SO_4 solution, both in the absence and presence of salts I and II, were simulated using the equivalent circuit model proposed in Figure 3.

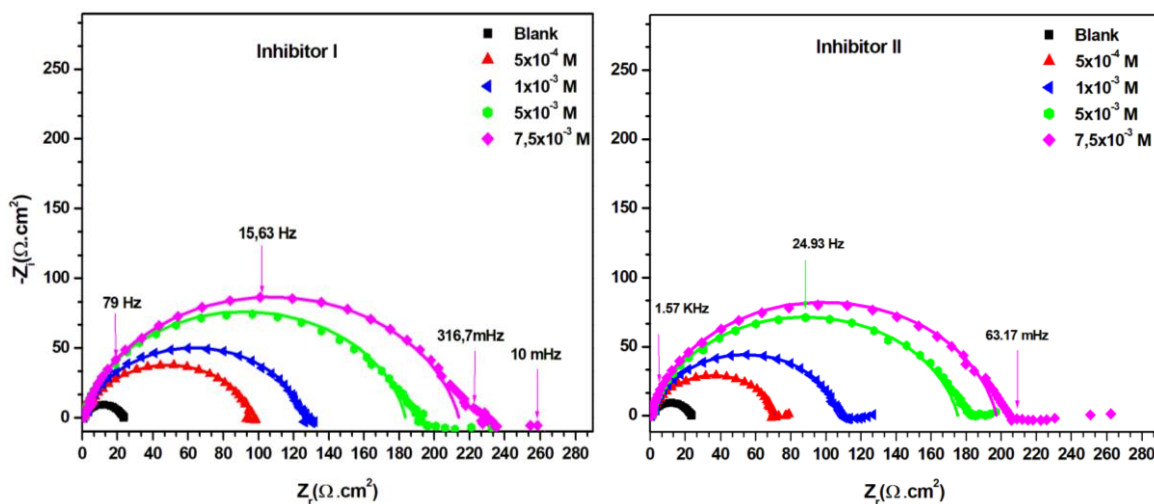


Figure 2. Nyquist plots of API 5L Grade B steel in 0.5 M H₂SO₄, without and with different concentration of pyridinium salts I and II at 25°C.

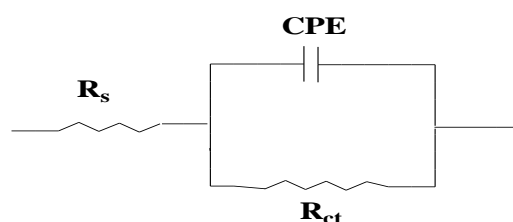


Figure 3. Proposed equivalent circuit model for the systems studied.

Here, R_s represents the solution resistance, R_{ct} denotes the charge transfer resistance, and CPE stands for the constant phase element. The use of the constant phase element, instead of a capacitor in the equivalent circuit schematic, was implemented to achieve a more precise fit. This adjustment was necessary because the metal/solution interface does not correspond to a conventional capacitor. The adoption of the constant phase element is a common practice aimed at accommodating deviations caused by the roughness of the metal surface [35]. The parameters values, including R_s , R_{ct} , Y_0 , n , obtained by fitting the EIS data using the equivalent circuit of Figure 3, are listed in Table 3. The double layer capacitance (C_{dl}) and the inhibition efficiency ($IE\%$) are respectively defined and calculated as follows [36, 37]:

$$C_{dl} = (Y_0 \times R_{ct}^{(1-n)})^{\frac{1}{n}} \quad (6)$$

$$IE = \frac{R_{ct(i)} - R_{ct}^0}{R_{ct}} \times 100 \quad (7)$$

where Y_0 is the proportionality factor; n is the electrode surface roughness/heterogeneity factor; $R_{ct(i)}$ and R_{ct}^0 are the charge transfer resistance values in the presence and absence of the inhibitor, respectively.

As indicated in Table 3, the R_{ct} values in the inhibited solution surpass those in the corrosive solution, indicating that the addition of inhibitors restrains the corrosion process. With an increase in the inhibitor concentration, the charge transfer resistance also rises significantly, suggesting a more effective blocking of the corrosion process at higher concentrations. Conversely, C_{dl} values decrease as the inhibitor concentration increases. This reduction in C_{dl} is attributed to a decrease in the local dielectric constant and an increase in the thickness of the double layer [38]. This behavior is commonly observed in systems where inhibitor molecules are absorbed, forming an adherent film on the metal surface [39, 40], indicating that these compounds effectively inhibit the corrosion of API 5L Grade B steel. The values of n , both in the absence and presence of inhibitors, approach unity, suggesting a nearly capacitive interface [41]. Additionally, the inhibition efficiencies obtained from EIS align well with those obtained through the weight loss method and polarization curves.

Table 3. The inhibition efficiencies and electrochemical impedance parameters for API 5L Grade B steel in 0.5 M H_2SO_4 solution without and with different concentrations of pyridinium salts at 25°C.

	C_{inh}, M	$R_s, \Omega \cdot cm^2$	$R_{ct}, \Omega \cdot cm^2$	CPE, n	$Y_0, s^n/cm^2 \cdot \Omega$	$C_{dl}, \mu F \cdot cm^{-2}$	$IE\%$
Blank	0	1,27	22.32	0.88	287.39×10^{-6}	144.36	–
Inhibitor I	5×10^{-4}	1.04	95.56	0.85	158.94×10^{-6}	75.91	76.64
	1×10^{-3}	1.06	124.49	0.86	137.73×10^{-6}	71.05	82.07
	5×10^{-3}	0.84	182.68	0.88	115.47×10^{-6}	68.22	87.78
	7.5×10^{-3}	1.02	212.92	0.87	93.16×10^{-6}	51.85	89.51
Inhibitor II	5×10^{-4}	0.91	70.35	0.87	162.26×10^{-6}	83.16	68.27
	1×10^{-3}	1.01	107.19	0.88	139.09×10^{-6}	78.38	79.17
	5×10^{-3}	0.89	173.73	0.87	101.88×10^{-6}	55.75	87.15
	7.5×10^{-3}	0.72	196.60	0.88	90.67×10^{-6}	52.35	88.64

3.5. Adsorption isotherms

Metal corrosion protection by organic compounds in acidic environments relies on the adsorption of inhibitor molecules onto the metal surface. Investigating the adsorption isotherm is crucial for understanding the interaction between the inhibitor molecules and the metal surface. In this research, various isotherms, including Langmuir, Temkin, and Frumkin, were plotted at 25°C using the θ values derived from the weight loss method. This approach aimed to identify the most suitable adsorption isotherm for the studied system.

The appropriate isotherm, which appears graphically as a straight line, was determined using the correlation coefficient (R^2). The Langmuir isotherm, which is shown in Figure 4, proved to be the best fit, with a correlation coefficient closest to 1 (0.999), indicating that

the adsorption of pyridinium salts I and II on the steel surface in 0.5 M H₂SO₄ medium follows the Langmuir adsorption isotherm.

The following equation describes the correlation between surface coverage (θ) and inhibitor concentration C_{inh} via the Langmuir isotherm.

$$\frac{C_{\text{inh}}}{\theta} = \frac{1}{K_{\text{ads}}} + C_{\text{inh}} \quad (8)$$

where C_{inh} is the concentration of inhibitor, K_{ads} is the equilibrium constant for the adsorption process, and θ is the surface coverage.

The equilibrium constant of the adsorption process (K_{ads}) is obtained from the inverse of the value of the intersection of the straight line with the X-axis. It is related to the standard free energy of adsorption, ΔG_{ads} , according to the following formula:

$$K = \frac{1}{55.5} \exp\left(-\frac{\Delta G_{\text{ads}}^0}{RT}\right) \quad (9)$$

where R is the gas constant and T is the absolute temperature (K). The value of 55.5 is the concentration of water in solution in $\text{mol} \cdot \text{L}^{-1}$ [42].

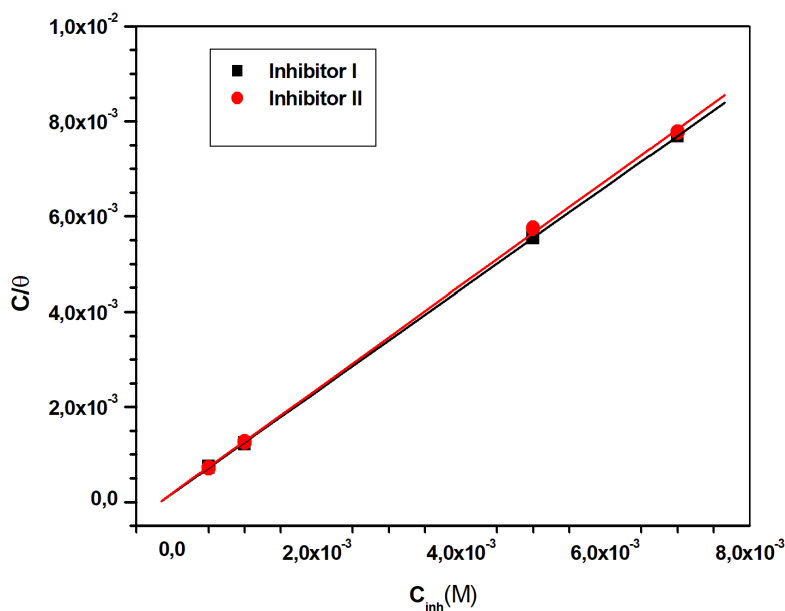


Figure 4. Langmuir adsorption isotherm plot for API 5L Grade B steel in 0.5 M H₂SO₄ solution containing different concentrations of pyridinium salts I and II at 25°C.

The values of ΔG_{ads} and K_{ads} are reported in Table 4. The negative values of ΔG_{ads} indicate the adsorption process's spontaneity and the adsorbed layer's stability on the metal surface. Generally, values of ΔG_{ads} close to $-20 \text{ kJ} \cdot \text{mol}^{-1}$ or lower are linked to electrostatic interactions between the charged molecules and the metal (physical adsorption). However, those close to $-40 \text{ kJ} \cdot \text{mol}^{-1}$ or higher involve a transfer of charges between the organic molecules and the metal surface (chemisorption) [43, 44]. According to Table 4, the

calculated ΔG_{ads} values fall within the range of $-20 \text{ kJ}\cdot\text{mol}^{-1}$ to $-40 \text{ kJ}\cdot\text{mol}^{-1}$. It looks like the two pyridinium salts adsorbed on the surface of API 5L Grade B steel in a way that is a mix of physical and chemical adsorption, not just one type [15, 45, 46].

Table 4. K_{ads} and ΔG_{ads} parameters for adsorption of pyridinium salts I and II on API 5L Grade B steel surface in 0.5 M H_2SO_4 solutions at 25°C.

Inhibitor	R^2	K_{ads}	$\Delta G_{\text{ads}} (\text{kJ}\cdot\text{mol}^{-1})$
Inhibitor I	0.999	5.50×10^3	-31.28
Inhibitor II	0.999	5.24×10^3	-31.16

3.6. Effect of temperature

The corrosion rate is significantly influenced by temperature, which plays a pivotal role in the electrochemical reactions that drive the corrosion process. Generally, an increase in temperature accelerates corrosion kinetics, which also affects the capacity and action of inhibitors [47, 48]. In order to determine the effect of this factor on the inhibition efficiency of the two pyridinium salts, gravimetric measurements were performed in 0.5 M H_2SO_4 solution without and with $7.5 \times 10^{-3} \text{ M}$ at 25–55°C with a 10°C interval for 2 hours of exposure. The results obtained are given in Table 5. It can be seen that when the temperature rises by 10°C, the corrosion rate increases, while this rise is lower in the presence of both inhibitors. Moreover, the increase in temperature positively affects the inhibition efficiency. The rise in IE (%) values with temperature suggests that the adsorption of the inhibitor molecules on the metal surface is chemical rather than physical [49].

Table 5. Corrosion rate and inhibition efficiency of API 5L Grade B steel in 0.5 M H_2SO_4 without and with $7.5 \times 10^{-3} \text{ M}$ of inhibitors at different temperatures.

Temperature (°C)	Blank ($W, \text{g}\cdot\text{h}^{-1}\cdot\text{m}^{-2}$)	Inhibitor I ($W, \text{g}\cdot\text{h}^{-1}\cdot\text{m}^{-2}$)	$IE, \%$	Inhibitor II ($W, \text{g}\cdot\text{h}^{-1}\cdot\text{m}^{-2}$)	$IE, \%$
25	9.77	0.87	91.10	0.92	90.57
35	18.30	1.39	92.40	1.54	91.58
45	36.40	2.29	93.70	2.55	92.99
55	69.30	4.01	94.21	4.19	93.95

3.6.1. Thermodynamic parameters of the corrosion process

The study of the evolution of the corrosion rate *versus* temperature permits the use of the Arrhenius equation (10) and transition state equation (11) to calculate some thermodynamic parameters of the corrosion process, such as the activation energy (E_a), the activation enthalpy (ΔH_a^0) and the activation entropy (ΔS_a^0).

$$\ln W = \ln K - \frac{E_a}{RT} \quad (10)$$

$$\ln \frac{W}{T} = \frac{RT}{Nh} + \left(\frac{\Delta S_a^0}{R} \right) - \left(\frac{\Delta H_a^0}{RT} \right) \quad (11)$$

where W is the corrosion rate, R is the universal gas constant, T is the absolute temperature (K), A is the pre-exponential factor, N is the Avogadro's number, h is the Plank's constant.

The Arrhenius plots of $\ln W$ against $1/T$ and the transition state $\ln(W/T)$ versus $1/T$ for API 5L Grade B steel in 0.5 M H_2SO_4 solution without and with 7.5×10^{-3} M of pyridinium salts I and II are shown in Figures 5 and 6, respectively.

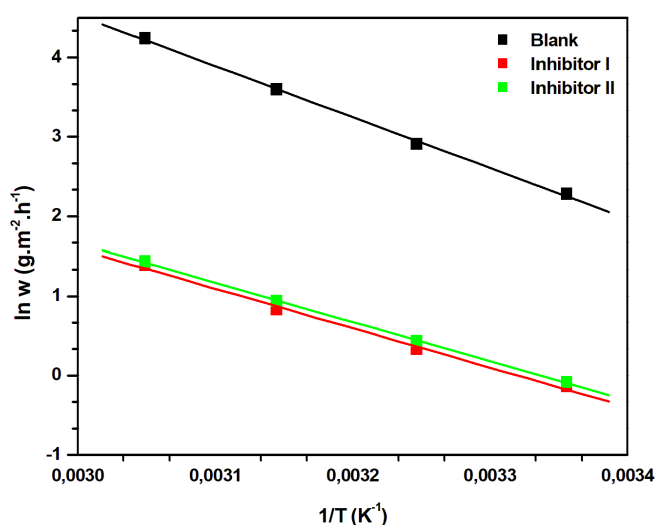


Figure 5. Arrhenius plots for API 5L Grade B steel in 0.5 M H_2SO_4 solution without and with 7.5×10^{-3} M of pyridinium salts I and II.

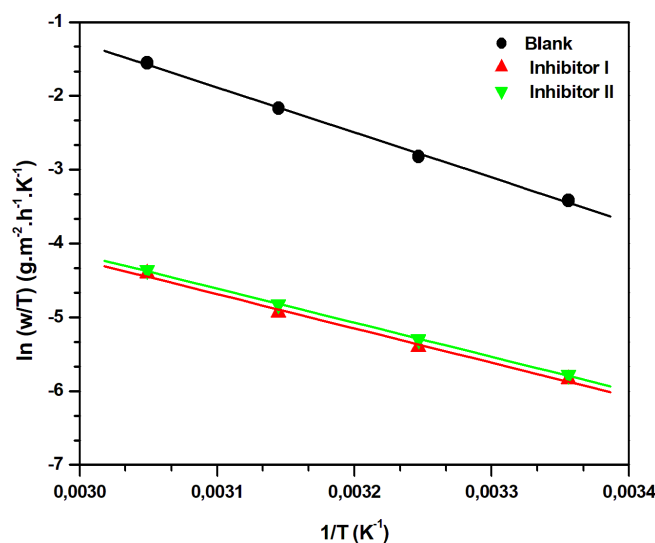


Figure 6. Transition state plots for API 5L Grade B steel in 0.5 M H_2SO_4 solution without and with 7.5×10^{-3} M of pyridinium salts I and II.

For the blank solution and both pyridinium salts, the linear regression coefficients are close to 1 (Table 6), which indicates that the corrosion of steel in 0.5 M H_2SO_4 can be described using the Arrhenius kinetic model. The values of the activation energies, enthalpies ΔH_a^0 , and entropies ΔS_a^0 are given in Table 6. With 7.5×10^{-3} M of inhibitors, the activation energy, enthalpy and entropy decrease, the decrease in activation energy may be attributed to the chemisorption of these inhibitors on the steel surface [50, 51]. Positive enthalpy values indicate that the metal dissolution process is endothermic. In the presence and absence of pyridinium salts, the entropy of activation displays a negative and essential value. It indicates that the activation complex observed during the rate-determining phase represents an association instead of a dissociation process. This suggests that the disorder during the transfer of the reactants to the activated complex was reduced [52].

Table 6. Thermodynamic parameters and linear regression coefficients for API 5L Grade B steel in 0.5 M H_2SO_4 solution without and with 7.5×10^{-3} M of pyridinium salts I and II.

Compound	R^2	E_a , $\text{kJ} \cdot \text{mol}^{-1}$	ΔH_a^0 , $\text{kJ} \cdot \text{mol}^{-1}$	ΔS_a^0 , $\text{kJ} \cdot \text{mol}^{-1}$
Blank	0.999	53.29	50.70	−55.99
Inhibitor I	0.997	41.23	38.66	−116.59
Inhibitor II	0.999	41.04	38.41	−116.70

3.7. Atomic force microscopy images

AFM images of steel samples before and after 4 hours of immersion in the absence and presence of 7.5×10^{-3} M of pyridinium salts I and II are shown in Figures 7a–d. When a steel sample is exposed to free H_2SO_4 , its surface exhibits a porous structure characterized by broad and deep pores resulting from the corrosive action of the acid. The addition of inhibitors led to apparent differences in the surface morphology of the specimens. The surface is more uniform in the presence of both inhibitors. Average surface roughness values (Table 7) obtained in the presence of pyridinium salts I (29.34 nm) and II (68.09 nm) are lower than those obtained in 0.5 M H_2SO_4 (98.20 nm). This indicates that the inhibitor molecules are adsorbed on the steel surface, thereby reducing the acid attack.

Table 7. Average surface roughness values API 5L Grade B steel (a) abraded, (b) in 0.5 M H_2SO_4 , (c), and (d) in the presence of 7.5×10^{-3} M of inhibitors I and II, respectively.

	a	b	c	d
Average surface roughness, nm	11.92	98.20	29.34	68.09

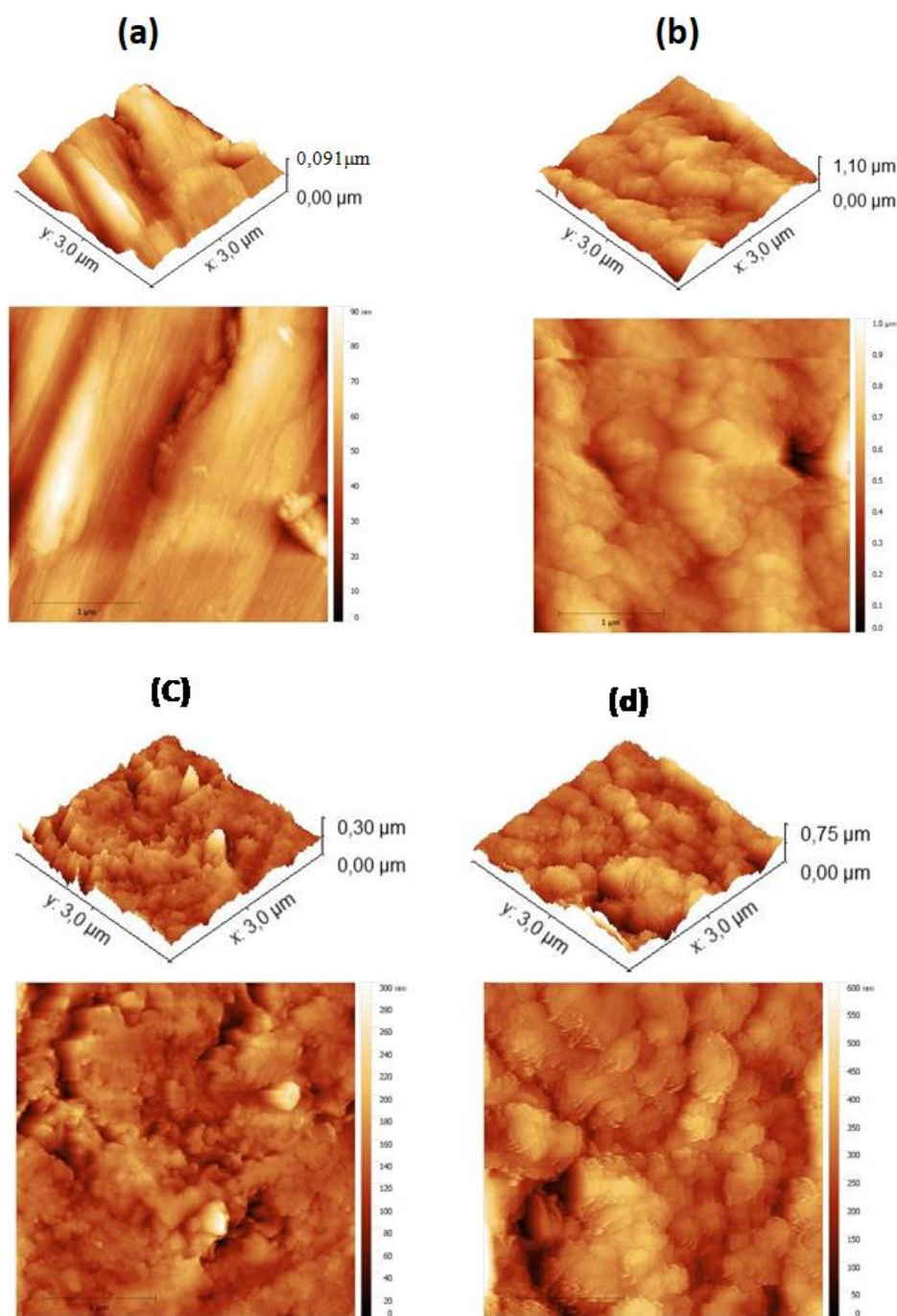


Figure 7. AFM images of API 5L Grade B steel (a) abraded, (b) in 0.5 M H_2SO_4 , (c), and (d) in the presence of 7.5×10^{-3} M of inhibitors I and II, respectively.

3.8. Quantum chemical calculations

In order to understand the influence of molecular structure on the inhibition efficiency of the compounds under investigation, quantum chemical calculations were conducted using the DFT method. The optimized geometrical structures, as well as the electron distribution in the lowest unoccupied molecular orbital (LUMO) and highest occupied molecular orbital

(HOMO) energy levels, are illustrated in Figure 8. Furthermore, the computed quantum chemical parameters, specifically E_{HOMO} , E_{LUMO} , ΔE , and the dipole moment (μ), are presented in Table 8.

For the two pyridinium salt derivatives, the HOMO is localized on the halide anions (Br^-), and the CH_2 , $\text{CH}_2\text{--CH}_2$ atoms that are seated between the pyridiniums ring, and this indicates that the inhibitors adsorb onto the steel surface via coordination sites present in these centers.

On the other hand, the LUMO is focused on all salt molecules. This means that both anionic and cationic entities can accept electrons from steel and can be adsorbed to their surfaces through electron retro-donation.

Generally, the ability of a molecule to donate electrons increases with the HOMO energy value. In contrast, a low LUMO energy value indicates that the molecule is more able to accept electrons [53]. Thus, the adsorption of an inhibitor and its corrosion inhibition performance is characterized by a high value of HOMO energy, a low value of LUMO energy, a low energy interval ΔE and a high value of dipole moment [54, 55]. Comparing the quantum parameters of pyridinium salts I and II shown in Table 8, pyridinium salt I has a low value of E_{LUMO} , a low energy interval ΔE , and a high value of dipole moment, perfectly consistent with the order of inhibition efficiency found by experimentation.

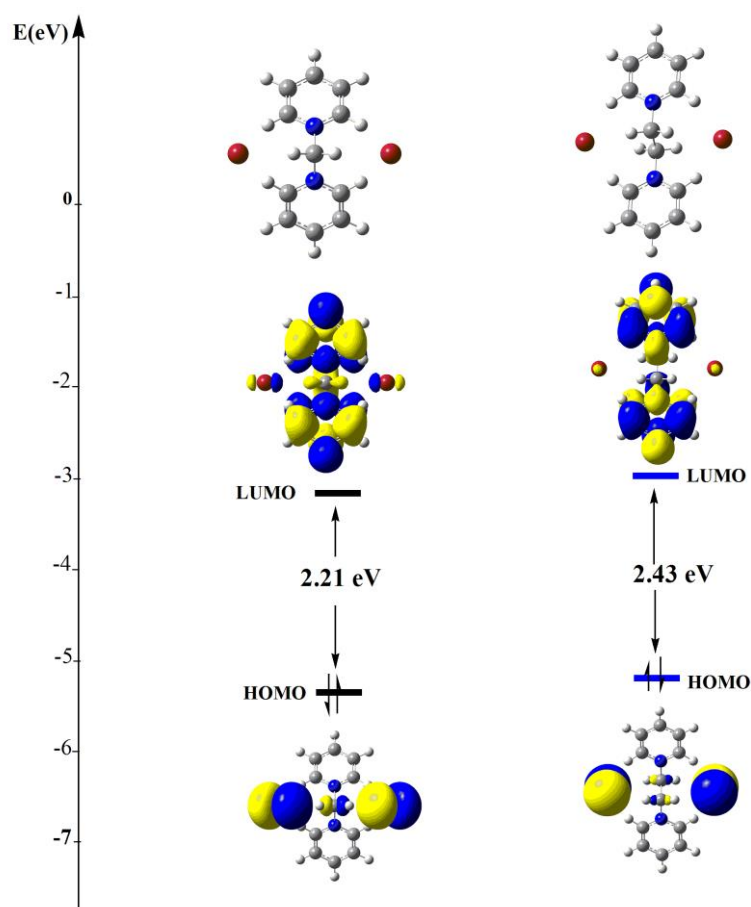


Figure 8. The HOMO and LUMO distributions of pyridinium salts I and II.

Table 8. E_{HOMO} , E_{LUMO} , ΔE , and the dipole moment (μ) for pyridinium salts I and II.

	E_{HOMO} , eV	E_{LUMO} , eV	ΔE_{gap} , eV	μ (D)
Inhibitor I	−5.425	−3.216	2.209	10.994
Inhibitor II	−5.235	−2.755	2.480	0.044

Conclusion

1. The three methods used in this study show that both pyridinium salts have good inhibiting properties against API 5L Grade B steel corrosion in sulfuric acid. Good agreement between the E (%) values calculated by the mass loss method, the polarization curves and EIS method.
2. The inhibition efficiency increases with the concentration of pyridinium salts and the temperature increase.
3. The polarization curves show that both pyridinium salts stop the anodic and cathodic processes of steel corrosion and are mixed-type inhibitors.
4. The EIS method showed that the charge transfer controls the corrosion process of steel in the absence and presence of both pyridinium salts.
5. The adsorption of both inhibitor obeys Langmuir's adsorption isotherm and occurs via electrostatic and chemical bonds.
6. AFM images confirm the protection of API 5L Grade B steel in 0.5 M H_2SO_4 solution by the studied pyridinium salts.

Acknowledgments

We sincerely thank Mr. Moussa MEZHOU for assisting us in conducting the AFM analyses.

References

1. R.W. Leonard, *Precoated steel sheet*, Metals Handbook, 10th edition, American Society for Metals, 1990, vol. 1, pp. 567–582.
2. X. Wang, Y. Wan, Y. Zeng and Y. Gu, Investigation of benzimidazole compound as a novel corrosion inhibitor for mild steel in hydrochloric acid solution, *Int. J. Electrochem. Sci.*, 2012, **7**, no. 3, 2403–2415. doi: [10.1016/S1452-3981\(23\)13888-0](https://doi.org/10.1016/S1452-3981(23)13888-0)
3. R. Yıldız, An electrochemical and theoretical evaluation of 4,6-diamino-2-pyrimidinethiol as a corrosion inhibitor for mild steel in HCl solutions, *Corros. Sci.*, 2015, **90**, 544–553. doi: [10.1016/j.corsci.2014.10.047](https://doi.org/10.1016/j.corsci.2014.10.047)
4. X. Li, S. Deng and X. Xie, Experimental and theoretical study on corrosion inhibition of oxime compounds for aluminium in HCl solution, *Corros. Sci.*, 2014, **81**, 162–175. doi: [10.1016/j.corsci.2013.12.021](https://doi.org/10.1016/j.corsci.2013.12.021)

-
5. N. Palaniappan, L.R. Chowhan, S. Jothi, I.G. Bosco and I.S. Cole, Corrosion inhibition on mild steel by phosphonium salts in 1 M HNO₃ aqueous medium, *Surf. Interfaces*, 2017, **6**, 237–246. doi: [10.1016/j.surfin.2016.10.003](https://doi.org/10.1016/j.surfin.2016.10.003)
 6. M. En-Nyly, S. Skal, Y. El Aoufir, H. Serrar, H. Lgaz, S. Boukhris, O. Benali, T. Guedira and H.-S. Lee, Elucidating the mechanisms of novel thiazole-based corrosion inhibitors in carbon steel/HCl interface: An integrated approach combining experimental and computational studies, *J. Mol. Struct.*, 2024, **1306**, 137317. doi: [10.1016/j.molstruc.2024.137817](https://doi.org/10.1016/j.molstruc.2024.137817)
 7. N.S. Abdelshafi, A.A. Farag, F.E.-T. Heakal, A.-S. Badran, K.M. Abdel-Azim, A.R. Manar El Sayed and M.A. Ibrahim, In-depth experimental assessment of two new aminocoumarin derivatives as corrosion inhibitors for carbon steel in HCl media combined with AFM, SEM/EDX, contact angle, and DFT/MDS simulations, *J. Mol. Struct.*, 2024, **1304**, 137638. doi: [10.1016/j.molstruc.2024.137638](https://doi.org/10.1016/j.molstruc.2024.137638)
 8. R. Tourir, N. Errahmany, M. Rbaa, F. Benhiba, M. Doubi, E.H. EL Kafssaoui and B. Lakhrissi, Experimental and computational chemistry investigation of the molecular structures of new synthetic quinazolinone derivatives as acid corrosion inhibitors for mild steel, *J. Mol. Struct.*, 2024, **1303**, 137499. doi: [10.1016/j.molstruc.2024.137499](https://doi.org/10.1016/j.molstruc.2024.137499)
 9. M. Galai, K. Dahmani, O. Kharbouch, M. Rbaa, N. Alzeqri, L. Guo, A.A. AlObaid, A. Hmada, N. Dkhireche, E. Ech-chihbi, M. Ouakki, M. Ebn Touhami and I. Warad, Surface analysis and interface properties of a newly synthesized quinoline-derivative corrosion inhibitor for mild steel in acid pickling bath: Mechanistic exploration through electrochemical, XPS, AFM, contact angle, SEM/EDS, and computational studies, *J. Phys. Chem. Solids*, 2024, **184**, 11169. doi: [10.1016/j.jpcs.2023.111681](https://doi.org/10.1016/j.jpcs.2023.111681)
 10. J. O'M. Bockris, A.K.N. Reddy and M. Gamboa-Aldeco, *Modern electrochemistry*, vol. 2A, 2nd edition, New York, Kluwer Academic Publishers, 2004, 1534 pp.
 11. S. Muralidharan, M.A. Quraishi and S.V.K. Iyer, The effect of molecular structure on hydrogen permeation and the corrosion inhibition of mild steel in acidic solutions, *Corros. Sci.*, 1995, **37**, no. 11, 1739–1750. doi: [10.1016/0010-938X\(95\)00068-U](https://doi.org/10.1016/0010-938X(95)00068-U)
 12. J. G. N. Thomas, Some new fundamental aspects in corrosion inhibitors, In: Proceedings of the 5th European Symposium on Corrosion Inhibitors, Ann Univ. Ferrara, Italy, 1981, vol. 8, p. 453.
 13. M.A. Hegazy, A.M. Badawi, S.S. Abd El Rehim and W.M. Kamel, Corrosion inhibition of carbon steel using novel *N*-(2-(2-mercaptoacetoxy) ethyl)-*N,N*-dimethyl dodecan-1-aminium bromide during acid pickling, *Corros. Sci.*, 2013, **69**, 110–122. doi: [10.1016/j.corsci.2012.11.031](https://doi.org/10.1016/j.corsci.2012.11.031)
 14. M.A. Hegazy, M. Abdallah, M.K. Awad and M. Rezk, Three novel di-quaternary ammonium salts as corrosion inhibitors for API X65 steel pipeline in acidic solution. Part I: Experimental results, *Corros. Sci.*, 2014, **81**, 54–64. doi: [10.1016/j.corsci.2013.12.010](https://doi.org/10.1016/j.corsci.2013.12.010)

-
15. S. Yesudass, L.O. Olasunkanmi, I. Bahadur, M.M. Kabandaa, I.B. Obot and E.E. Ebenso, Experimental and theoretical studies on some selected ionic liquids with different cations/anions as corrosion inhibitors for mild steel in acidic medium, *J. Taiwan Inst. Chem. Eng.*, 2016, **64**, 252–268. doi: [10.1016/j.jtice.2016.04.006](https://doi.org/10.1016/j.jtice.2016.04.006)
 16. X. Zheng, S. Zhang, W. Li, L. Yin, J. He and J. Wu, Investigation of 1-butyl-3-methyl-1*H*-benzimidazolium iodide as inhibitor for mild steel in sulfuric acid solution, *Corros. Sci.*, 2014, **80**, 383–392. doi: [10.1016/j.corsci.2013.11.053](https://doi.org/10.1016/j.corsci.2013.11.053)
 17. K. Shalabi, A.M. Helmy, A.H. El-Askalany and M.M. Shahba, New pyridinium bromide mono-cationic surfactant as corrosion inhibitor for carbon steel during chemical cleaning: Experimental and theoretical studies, *J. Mol. Liq.*, **293**, 2019, 111480. doi: [10.1016/j.molliq.2019.111480](https://doi.org/10.1016/j.molliq.2019.111480)
 18. F. El-Hajjaji, S. Rajae, M. Mouslim, M.V.M. de Yuso, E. Rodríguez-Castellón, S.M. Almutairi, M. Taleb, S. Jodeh and M. Algarra, Insights of Corrosion Inhibitor Based in Pyridinium Ionic Liquids, *Arabian J. Sci. Eng.*, **48**, 2023, 7755–7770. doi: [10.1007/s13369-022-07502-0](https://doi.org/10.1007/s13369-022-07502-0)
 19. F. EL Hajjaji, R. Salim, M. Taleb, F. Benhiba, N. Rezki, D.S. Chauhan and M.A. Quraishi, Pyridinium-based ionic liquids as novel eco-friendly corrosion inhibitors for mild steel in molar hydrochloric acid: Experimental & computational approach, *Surf. Interfaces*, **22**, 2021, 100881. doi: [10.1016/j.surfin.2020.100881](https://doi.org/10.1016/j.surfin.2020.100881)
 20. S. Zhang, Z. Tao, S. Liao and F. Wu, Substitutional adsorption isotherms and corrosion inhibitive properties of some oxadiazol-triazole derivative in acidic solution, *Corros. Sci.*, 2010, **52**, 3126–3132. doi: [10.1016/j.corsci.2010.05.035](https://doi.org/10.1016/j.corsci.2010.05.035)
 21. S. Deng, X. Li and H. Fu, Triazolyl blue tetrazolium bromide as a novel corrosion inhibitor for steel in HCl and H₂SO₄ solutions, *Corros. Sci.*, 2011, **53**, no. 1, 302. doi: [10.1016/j.corsci.2010.09.036](https://doi.org/10.1016/j.corsci.2010.09.036)
 22. S. Deng, X. Li and H. Fu, Alizarin, violet 3B as a novel corrosion inhibitor for steel in HCl, H₂SO₄ solutions, *Corros. Sci.*, 2011, **53**, no. 11, 3596–3602. doi: [10.1016/j.corsci.2011.07.003](https://doi.org/10.1016/j.corsci.2011.07.003)
 23. A. Nikitasari, G. Priyotomo, S. Prifiarni, S. Musabikha, R. Kusumastuti, J. Triwardono, P.D.N. Lotulung, S. Bahtiar, E. Yanuar, L. Suhaimi, R. Desiasni and F. Widyawati, Anti-corrosion inhibition of API 5L in hydrochloric acid solution by ethanol extract of *Phyllanthus niruri* leaf, *Int. J. Corros. Scale Inhib.*, 2024, **13**, no. 1, 1–20. doi: [10.17675/2305-6894-2024-13-1-1](https://doi.org/10.17675/2305-6894-2024-13-1-1)
 24. V.I. Jasmine, P.S.L.M. Kala, M.J. Clara, H.M. Banu, A. Nirmala, N. Anitha, A. Krishnaveni and S. Rajendran, Electrochemical studies on emulsion coated mild steel in ground water, *Int. J. Corros. Scale Inhib.*, 2024, **13**, no. 1, 542–566. doi: [10.17675/2305-6894-2024-13-1-27](https://doi.org/10.17675/2305-6894-2024-13-1-27)
 25. A.A. Aksüt, W.J. Lorenz and F. Mansfeld, The determination of corrosion rates by electrochemical d.c. and a.c. Methods II. Systems with discontinuous steady state polarization behavior, *Corros. Sci.*, 1982, **22**, no. 7, 611–619. doi: [10.1016/0010-938X\(82\)90042-7](https://doi.org/10.1016/0010-938X(82)90042-7)

-
26. B.G. Ateya, B.M. Abo-Elkhair and I.A. Abdel-Hamid, Thiosemicarbazide as an inhibitor for the acid corrosion of iron, *Corros. Sci.*, 1976, **16**, no. 3, 163–169. doi: [10.1016/0010-938X\(76\)90057-3](https://doi.org/10.1016/0010-938X(76)90057-3)
 27. Y. Abboud, A. Abourriche, T. Saffaj, M. Berrada, M. Charrouf, A. Bennamara, A. Cherqaoui and D. Takky, The inhibition of mild steel corrosion in acidic medium by 2,2'-bis(benzimidazole), *Appl. Surf. Sci.*, 2006, **252**, no. 23, 8178–8184. doi: [10.1016/j.apsusc.2005.10.060](https://doi.org/10.1016/j.apsusc.2005.10.060)
 28. A.K. Satapathy, G. Gunasekaran, S.C. Sahoo, K. Amit and P.V. Rodrigues, Corrosion inhibition by Justicia gendarussa plant extract in hydrochloric acid solution, *Corros. Sci.*, 2009, **51**, no. 12, 2848–2858. doi: [10.1016/j.corsci.2009.08.016](https://doi.org/10.1016/j.corsci.2009.08.016)
 29. X. Li, S. Deng and F. Hui, Triazolyl blue tetrazolium bromide as a novel corrosion inhibitor for steel in HCl and H₂SO₄ solutions, *Corros. Sci.*, 2011, **53**, no. 1, 302–309. doi: [10.1016/j.corsci.2010.09.036](https://doi.org/10.1016/j.corsci.2010.09.036)
 30. A. Döner, R. Solmaz, M. Özcan and G. Kardas, Experimental and theoretical studies of thiazoles as corrosion inhibitors for mild steel in sulphuric acid solution, *Corros. Sci.*, 2011, **53**, no. 9, 2902–2913. doi: [10.1016/j.corsci.2011.05.027](https://doi.org/10.1016/j.corsci.2011.05.027)
 31. K.S. Jacob and G. Parameswaran, Corrosion inhibition of mild steel in hydrochloric acid solution by schiff base furoin thiosemicarbazone, *Corros. Sci.*, 2010, **52**, no. 1, 224–228. doi: [10.1016/j.corsci.2009.09.007](https://doi.org/10.1016/j.corsci.2009.09.007)
 32. M.H. Hussin and M.J. Kassim, The corrosion inhibition and adsorption behavior of uncaria gambir extract on mild steel in 1M HCl, *Mater. Chem. Phys.*, 2011, **125**, no. 3, 461–468. doi: [10.1016/j.matchemphys.2010.10.032](https://doi.org/10.1016/j.matchemphys.2010.10.032)
 33. A. Döner and G. Kardas, N-Aminorhodanine as an effective corrosion inhibitor for mild steel in 0.5M H₂SO₄, *Corros. Sci.*, 2011, **53**, no. 12, 4223–4232. doi: [10.1016/j.corsci.2011.08.032](https://doi.org/10.1016/j.corsci.2011.08.032)
 34. R. Solmaz, E. Altunbas and G. Kardas, Adsorption and corrosion inhibition effect of 2-((5-mercapto-1,3,4-thiadiazol-2-ylimino)methyl)phenol Schiff base on mild steel, *Mater. Chem. Phys.*, 2011, **125**, no. 3, 796–801. doi: [10.1016/j.matchemphys.2010.09.056](https://doi.org/10.1016/j.matchemphys.2010.09.056)
 35. E. Barsoukov and Dr. J.R. Macdonald, *Impedance Spectroscopy: Theory, Experiment, and Applications*, 2nd Ed., John Wiley & Sons, Inc, Hoboken, New Jersey, New York, 2005, p. 13.
 36. H. Ma, X. Cheng, G. Li, S. Chen, Z. Quan, S. Zhao and L. Niu, The influence of hydrogen sulfide on corrosion of iron under different conditions, *Corros. Sci.*, 2000, **42**, no. 10, 1669–1683. doi: [10.1016/S0010-938X\(00\)00003-2](https://doi.org/10.1016/S0010-938X(00)00003-2)
 37. A. Popova, M. Christov and A. Vasilev, Inhibitive properties of quaternary ammonium bromides of N-containing heterocycles on acid mild steel corrosion. Part II: EIS results, *Corros. Sci.*, 2007, **49**, no. 8, 3290–3302. doi: [10.1016/j.corsci.2007.03.012](https://doi.org/10.1016/j.corsci.2007.03.012)
 38. M. McCafferty and N. Hackerman, Double layer capacitance of iron and corrosion inhibition with polymethylene diamines, *J. Electrochem. Soc.*, 1972, **119**, no. 2, 146–154. doi: [10.1149/1.2404150](https://doi.org/10.1149/1.2404150)

-
39. K.C. Emregül and O. Atakol, Corrosion inhibition of iron in 1M HCl solution with Schiff base compounds and derivatives, *Mater. Chem. Phys.*, 2004, **83**, no. 2–3, 373–379. doi: [10.1016/j.matchemphys.2003.11.008](https://doi.org/10.1016/j.matchemphys.2003.11.008)
40. I.L. Rosenfield, *Corrosion Inhibitors*, New York, McGraw-Hill, 1981, 327 pp.
41. M.G. Hosseini, S.F.L. Mertens, M. Ghorbani and M.R. Arshadi, Asymmetrical Schiff bases as inhibitors of mild steel corrosion in sulphuric acid media, *Mater. Chem. Phys.*, 2003, **78**, no. 3, 800–808. doi: [10.1016/S0254-0584\(02\)00390-5](https://doi.org/10.1016/S0254-0584(02)00390-5)
42. J. Flis and T. Zarkroczymski, Impedance study of reinforcing steel in simulated pore solution with tannin, *J. Electrochem. Soc.*, 1996, **143**, 2458–2464. doi: [10.1149/1.1837031](https://doi.org/10.1149/1.1837031)
43. Z. Szklarska-Smialowska and J. Mankowski, Crevice corrosion of stainless steels in sodium chloride solution, *Corros. Sci.*, 1978, **18**, no. 11, 953–960. doi: [10.1016/0010-938X\(78\)90030-6](https://doi.org/10.1016/0010-938X(78)90030-6)
44. A. Yurt, S. Ulutas and H. Dal, Electrochemical and theoretical investigation on the corrosion of aluminium in acidic solution containing some Schiff bases, *Appl. Surf. Sci.*, 2006, **253**, no. 2, 919–925. doi: [10.1016/j.apsusc.2006.01.026](https://doi.org/10.1016/j.apsusc.2006.01.026)
45. M.A.M. Ibrahim, M. Messali, Z. Moussa, A. Alzahrani, S.N. Alamry and B. Hammouti, Corrosion inhibition of carbon steel by imidazolium and pyridinium cations ionic liquids in acidic environment, *Port. Electrochim. Acta.*, 2011, **29**, no. 6, 375–389. doi: [10.4152/pea.201106375](https://doi.org/10.4152/pea.201106375)
46. M.E. Said, H. Allal, B. Mezhoud, M. Bouchouit, A. Chibani and A. Bouraiou, Experimental and theoretical evaluation of (iso) quinolinium bromide derivatives as corrosion inhibitors of steel E24 in 0.5M H₂SO₄ solution, *Int. J. Corros. Scale Inhib.*, 2023, **12**, no. 2, 679–695. doi: [10.17675/2305-6894-2023-12-2-16](https://doi.org/10.17675/2305-6894-2023-12-2-16)
47. M.A. Hegazy, M. Abdallah, M.K. Awad and M. Rezk, Three novel di-quaternary ammonium salts as corrosion inhibitors for API X65 steel pipeline in acidic solution. Part I: Experimental results, *Corros. Sci.*, 2014, **81**, 54–64. doi: [10.1016/j.corsci.2013.12.010](https://doi.org/10.1016/j.corsci.2013.12.010)
48. M. Yadav, S. Kumar, T. Purkait, L.O. Olasunkanmi, I. Bahadur and E.E. Ebenso, Electrochemical, thermodynamic and quantum chemical studies of synthesized benzimidazole derivatives as corrosion inhibitors for N80 steel in hydrochloric acid, *J. Mol. Liq.*, 2016, **213**, 122–138. doi: [10.1016/j.molliq.2015.11.018](https://doi.org/10.1016/j.molliq.2015.11.018)
49. A. Khadiri, R. Saddik, K. Bekkouche, A. Aouniti, B. Hammouti, N. Benchat, M. Bouachrine and R. Solmaz, Gravimetric, electrochemical and quantum chemical studies of some pyridazine derivatives as corrosion inhibitors for mild steel in 1 M HCl solution, *J. Taiwan Inst. Chem. Eng.*, 2016, **58**, 552–564. doi: [10.1016/j.jtice.2015.06.031](https://doi.org/10.1016/j.jtice.2015.06.031)
50. A.K. Satpati and P.V. Ravindran, Electrochemical study of the inhibition of corrosion of stainless steel by 1,2,3-benzotriazole in acidic media, *Mater. Chem. Phys.*, 2008, **109**, no. 2–3, 352–359. doi: [10.1016/j.matchemphys.2007.12.002](https://doi.org/10.1016/j.matchemphys.2007.12.002)

-
51. M. Lagrenee, B. Mernari, M. Bouanis, M. Traisnel and F. Bentiss, Study of the mechanism and inhibiting efficiency of 3,5-bis(4-methylthiophenyl)-4H-1,2,4-triazole on mild steel corrosion in acidic media, *Corros. Sci.*, 2002, **44**, no. 3, 573–588. doi: [10.1016/S0010-938X\(01\)00075-0](https://doi.org/10.1016/S0010-938X(01)00075-0)
52. S.S.A. El-Rehim, S.A.M. Refaey, F. Taha, M.B. Saleh and R.A. Ahmed, Corrosion inhibition of mild steel in acidic medium using 2-amino thiophenol and 2-cyanomethyl benzothiazole, *J. Appl. Electrochem.*, 2001, **31**, 429–435. doi: [10.1023/A:1017592322277](https://doi.org/10.1023/A:1017592322277)
53. J. Fang and J. Li, Quantum chemistry study on the relationship between molecular structure and corrosion inhibition efficiency of amides, *J. Mol. Struct.: THEOCHEM*, 2002, **593**, no. 1–3, 179–185. doi: [10.1016/S0166-1280\(02\)00316-0](https://doi.org/10.1016/S0166-1280(02)00316-0)
54. C.M. Goulart, A. Esteves-Souza, C.A. Martinez-Huitle, C.J.F. Rodrigues, M.A.M. Maciel and A. Echevarria, Experimental and theoretical evaluation of semicarbazones and thiosemicarbazones as organic corrosion inhibitors, *Corros. Sci.*, 2013, **67**, 281–291. doi: [10.1016/j.corsci.2012.10.029](https://doi.org/10.1016/j.corsci.2012.10.029)
55. A. Mohammed, H.S. Aljibori, M.A.I. Al-Hamid, W.K. Al-Azzawi, A.A.H. Kadhum and A. Alamiery, *N*-Phenyl-*N'*-[5-phenyl-1,2,4-thiadiazol-3-yl]thiourea: corrosion inhibition of mild steel in 1 M HCl, *Int. J. Corros. Scale Inhib.*, 2024, **13**, no. 1, 38–78. doi: [10.17675/2305-6894-2024-13-1-3](https://doi.org/10.17675/2305-6894-2024-13-1-3)

